Proc. Natl. Acad. Sci. USA
Vol. 91, pp. 3289–3293, April 1994
Physiology

Modulation of cardiac Na^+ channels expressed in a mammalian cell line and in ventricular myocytes by protein kinase C

(protein phosphorylation/ion channels/electrical excitability)

YUSHENG QU, JOHN ROGERS, TIMOTHY TANADA, TODD SCHEUER, AND WILLIAM A. CATTERALL

Department of Pharmacology, SJ-30, University of Washington, Seattle, WA 98195

Contributed by William A. Catterall, November 15, 1993

ABSTRACT **Cardiac rH1 Na^+ channel α subunits were expressed in cells of the Chinese hamster lung 1610 cell line by transfection, and a stable cell line expressing cardiac Na^+ channels (SNa-rH1) was isolated. Mean Na^+ currents of 2.2 ± 1.0 nA were recorded, which corresponds to a cell surface density of approximately 1–2 channels active at the peak of the Na^+ current per μm^2. The expressed cardiac Na^+ current was tetrodotoxin resistant (K_d = 1.8 μM) and had voltage-dependent properties similar to those of the Na^+ current in neonatal ventricular myocytes. Activation of protein kinase C by 1-oleoyl-2-acetyl-*sn*-glycerol (OAG) (10 μM) decreased this current ≈33% at a holding potential of −114 mV and 56% at −94 mV. This reduction in peak current was caused in part by an 8- to 14-mV shift of steady-state inactivation in the hyperpolarized direction. Na^+ channel activation was unchanged. Effects of OAG in SNa-rH1 cells and in neonatal rat cardiac myocytes were similar, except that the time course of inactivation was slowed either transiently or persistently when protein kinase C was activated in myocytes bathed in low-Ca^{2+} (1 μM) or Ca^{2+}-free solution but was unaffected in SNa-rH1 cells. The effects of OAG on cardiac Na^+ current were blocked in cells that had been previously microinjected with a peptide inhibitor of protein kinase C but not with a peptide inhibitor of cAMP-dependent protein kinase, indicating that protein kinase C is responsible for the effects of OAG. Single-channel recordings from SNa-rH1 cells showed that the probability of channel opening was reduced by OAG, but the conductance was unaffected. OAG did not induce the late Na^+ channel openings observed with PKC modulation of neuronal and skeletal muscle Na^+ channels. Thus, the substantial reduction in Na^+ current at normal diastolic depolarizations with 10 μM OAG is due to failure of channel opening in response to depolarization. Such Na^+ current reductions may have profound effects on cardiac cell excitability.**

The rapid upstroke of the cardiac action potential due to the Na^+ current through voltage-dependent Na^+ channels is responsible for the rapid spread of activation through the atria and ventricles that initiates and coordinates contraction of the heart. Cardiac function depends critically on the amplitude, timing, and voltage dependence of the Na^+ current, and interventions that modulate Na^+ current have potent physiological effects. The functional properties of mammalian cardiac Na^+ channels are distinctive. They are less sensitive to tetrodotoxin (TTX) than most Na^+ channels, with a K_d of approximately 1–10 μM (1), and their kinetics of activation and inactivation are slower and more complex (2). These properties are mediated by a distinct Na^+ channel α subunit (rH1) that was originally characterized by cloning from newborn rat heart (3) and denervated rat skeletal muscle (4). A closely related Na^+ channel has been described in human cardiac muscle (5). Expression of these α subunit cDNAs in *Xenopus* oocytes (5–7) yields Na^+ currents with functional properties and TTX sensitivity characteristic of the principal cardiac Na^+ channel.

Activation of protein kinase C (PKC) modulates Na^+ currents in neuroblastoma cells, rat brain neurons and skeletal muscle cells, *Xenopus* oocytes expressing rat brain mRNA or mRNA encoding type IIA Na^+ channel α subunits, and mammalian cells expressing type IIA α subunits (8–13). For sodium channels in rat brain neurons and skeletal muscle cells and for type IIA α subunits expressed in mammalian cells, inactivation of the sodium current is slowed and peak sodium current is reduced substantially (9, 10). Both slowing of inactivation and reduction of peak Na^+ current are prevented by mutation of serine-1506 in the inactivation gate of the rIIA Na^+ channel to alanine (14). This serine and its associated consensus sequence for PKC phosphorylation are conserved in the rH1 Na^+ channel (3), suggesting that similar modulation might occur in cardiac muscle. In this report, we describe the stable expression of the rH1 Na^+ channel in a mammalian cell line and characterize PKC modulation of cardiac Na^+ channels. We find that Na^+ current is sharply decreased after PKC activation at physiologically relevant diastolic membrane potentials, suggesting that phosphorylation of Na^+ channels by PKC may have dramatic effects on cardiac function.

EXPERIMENTAL PROCEDURES

Cell Culture. Cultured neonatal rat ventricular myocytes were prepared from 2-day-old newborn male rats by trypsin (Worthington) dispersion (15). Myocytes were seeded on sterile glass coverslips coated with 1% collagen and cultured in Dulbecco's modified Eagle's medium (DMEM; GIBCO) containing 15% horse serum, 5% fetal bovine serum, penicillin at 20 μg/ml, streptomycin at 10 μg/ml, and gentamycin at 60 μg/ml. Cells were maintained at 37°C in a 5% CO_2 incubator and used for experiments after 2–5 days in culture. SNa-rH1 cells and untransfected R1610 cells were maintained as described (16) and seeded on sterile plastic coverslips for recording.

Production of the SNa-rH1 Cell Line. cDNAs encoding the rH1 Na^+ channel α subunit were isolated by polymerase chain reaction using primers designed from the rH1 sequence (3) (J.R., T.T., and W.A.C., unpublished results). The cDNAs were sequenced and ligated to produce a full-length rH1 clone, and the full-length clone was subcloned into the pCDNA-3 vector (Invitrogen) to produce pCDNA-3/rH1-1. Chinese hamster lung 1610 cells (American Type Culture Collection) were transfected with pCDNA-3/rH1-1 by liposome-mediated transfection with *N*-[1-(2,3-dioleoyloxy)propyl]-*N,N,N*-trimethylammonium methyl sulfate (DOTAP; Boehringer Mann-

The publication costs of this article were defrayed in part by page charge payment. This article must therefore be hereby marked "*advertisement*" in accordance with 18 U.S.C. §1734 solely to indicate this fact.

Abbreviations: TTX, tetrodotoxin; PKC, protein kinase C; OAG, 1-oleoyl-2-acetyl-*sn*-glycerol; PKI, cAMP-dependent protein kinase inhibitor; PKCI, PKC inhibitor.

heim), and transfected cells were isolated by selection in the presence of G418 at 400 μg/ml. Single-cell clones were isolated and expanded, and the SNa-rH1 cell line was selected for further study by measurements of rH1 mRNA by Northern blotting and Na^+ currents by whole-cell voltage clamp.

Electrophysiological Recordings. Whole-cell and cell-attached voltage-clamp experiments (17) were performed at 22°C as described previously (9). Solutions for whole-cell experiments contained (in mM) 140 CsCl, 10 NaCl, 1 $MgCl_2$, 10 CsEGTA, 5 MgATP, 5 phosphocreatine (di-Tris salt), 0.2 GTP (Na^+ salt), and 10 Hepes in the pipette and 140 NaCl, 5 CsCl, 1.8 $CaCl_2$, 1 $MgCl_2$, 10 glucose, and 10 Hepes in the bath. Cell-attached experiments were conducted in either high-Ca^{2+}, high-Cl^- solutions containing 150 NaCl, 0.5 $CaCl_2$, 2 $MgCl_2$, and 5 Hepes in the pipette and 140 KCl, 10 NaCl, 0.5 $CaCl_2$, 3 $MgCl_2$, and 5 Hepes in the bath (pH adjusted to 7.4 with HCl) or low-Ca^{2+}, low-Cl^- solutions containing 150 $NaCH_3SO_3$, 1 $CaCl_2$, 2 $MgCl_2$, and 10 Hepes in the pipette and 140 KCH_3SO_3, 10 $NaCH_3SO_3$, 1 mM or 10 μM $CaCl_2$, 1.15 EGTA, 3 $MgCl_2$, and 10 Hepes in the bath (pH adjusted to 7.4 with CH_3SO_3H). Peptide inhibitors of cAMP-dependent protein kinase (PKI 5-24, Peninsula Laboratories) and PKC (PKCI 19-36, Peninsula Laboratories) were dissolved to make 1 mM PKI and 500 μM PKCI in the low-Ca^{2+}, low-Cl^- bath solution. 1-Oleoyl-2-acetyl-*sn*-glycerol (OAG; Sigma) was dissolved in dimethyl sulfoxide at concentrations of 1 or 10 mM and stored at −20°C until use.

All voltages have been corrected for liquid junction potentials. Conductance–voltage (g–V) relationships were calculated from peak current versus voltage (I–V) relationships according to $g = I/(V - V_r)$, where I is the peak current measured at voltage V and V_r is the measured reversal potential. Normalized conductance–voltage relationships and inactivation curves were fit with a Boltzmann distribution, $1/(1 + \exp[(V - V_{1/2})/k])$, where $V_{1/2}$ is the voltage of half activation or inactivation and k is a slope factor. Pooled data are reported as means and SEM in the text and figure legends. Statistical comparisons were made by using Student's t test, and P values are given in the text.

RESULTS AND DISCUSSION

Electrophysiological Comparison of Na^+ Channels in Cardiac Myocytes and in Cells Expressing rH1 Na^+ Channels. Membrane currents due to the rH1 Na^+ channel stably expressed in the Chinese hamster lung 1610 cell line (SNa-rH1 cells) were compared with those recorded in ventricular myocytes from neonatal rats by using the whole-cell and cell-attached recording configurations of the patch clamp technique (17). Large whole-cell Na^+ currents were observed in every SNa-rH1 cell (Fig. 1*A*), but they were not observed in untransfected cells. These currents were blocked 7.4 ± 6.7% by 100 nM TTX, 52.9 ± 13.4% by 2 μM TTX, and 90.8 ± 10.6% by 50 μM TTX (n = 4; data not shown), consistent with a K_d for TTX of 1.78 μM. A similar K_d of 1.98 μM was determined in the cultured ventricular myocytes. This TTX sensitivity is characteristic of cardiac Na^+ channels. The peak amplitude of Na^+ current expressed in SNa-rH1 cells ranged from 0.8 nA to 3.8 nA with a mean value of 2.2 ± 1.0 nA (n = 9) compared with 3.7 ± 1.6 nA (n = 6) for cultured ventricular myocytes. The membrane capacitance for SNa-rH1 cells was 29.1 ± 7.9 pF (n = 9). This corresponds to a channel density of 1–2 Na^+ channels per μm^2 in SNa-rH1 cells which may be compared with 2 channels per μm^2 in rat ventricular myocytes (18). Thus, rH1 Na^+ channels with appropriate TTX sensitivity are expressed efficiently in SNa-rH1 cells.

To compare the kinetics of the Na^+ currents recorded in the whole-cell voltage-clamp configuration, we superimposed traces of Na^+ currents elicited by depolarizations to

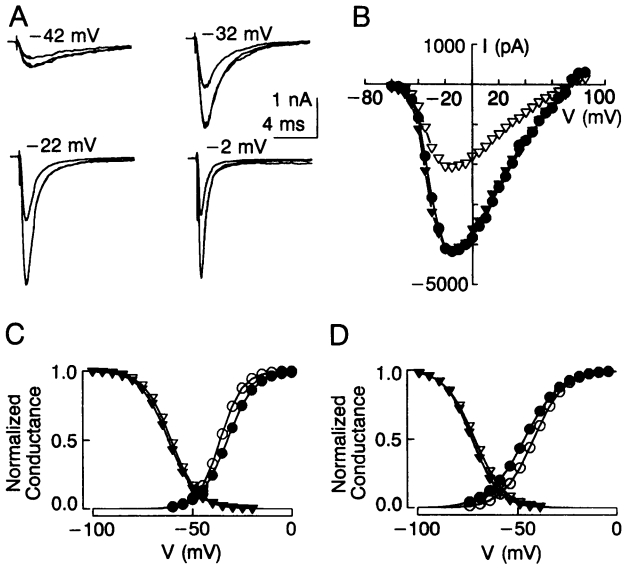

FIG. 1. Comparison of Na^+ currents in SNa-rH1 cells and neonatal rat ventricular myocytes. (*A*) Na^+ current traces in response to pulses to the indicated potentials. Three traces are plotted for each voltage: SNa-rH1 cell (larger currents), ventricular myocytes (smaller currents), and a scaled version of the myocyte current. Scaling factors were 1.5 for −42 mV, 1.8 for −32 mV, 2.0 for −22 mV, and 2.1 for −2 mV. The holding potential was −122 mV. (*B*) Current–voltage relationships for Na^+ current in the same cells as in *A*. ●, SNa-rH1; ▽, ventricular myocytes; ▼, ventricular myocytes × 2.0. (*C*) Average normalized conductance–voltage relationships determined by whole-cell voltage clamp recording gave the following mean values: SNa-rH1 cells, $V_{1/2}$ = −32.4 ± 3.7 mV and k = −6.7 ± 0.5 mV (n = 4); ventricular myocytes, $V_{1/2}$ = −36.0 ± 8.2 mV and k = −5.0 ± 1.8 mV (n = 5). Steady-state inactivation curves determined using a 98-ms conditioning pulse followed by a test pulse to −22 mV gave the following mean values: SNa-rH1 cells, $V_{1/2}$ = −61.9 ± 3.3 mV and k = 6.8 ± 0.6 mV (n = 4); ventricular myocytes, $V_{1/2}$ = −60.5 ± 6.2 mV and k = 6.6 ± 1.8 mV (n = 5). The mean values were used to construct the curves plotted. Filled symbols, SNa-rH1; open symbols, ventricular myocytes. (*D*) Average normalized conductance–voltage relationships and steady-state inactivation curves for cell-attached patch recording. Data were analyzed as for *C*. The mean values for conductance–voltage curves were SNa-rH1 cells, $V_{1/2}$ = −46.7 ± 3.9 mV and k = −8.9 ± 1.7 mV (n = 8); and ventricular myocytes, $V_{1/2}$ = −42.1 ± 5.5 mV and k = −7.7 ± 1.2 mV (n = 7). The mean values for the voltage dependence of steady-state inactivation were SNa-rH1 cells, $V_{1/2}$ = −72.6 ± 7.1 mV and k = 6.6 ± 1.7 mV (n = 8); ventricular myocytes, $V_{1/2}$ = −71.2 ± 3.5 mV and k = 7.2 ± 1.6 mV (n = 5). Filled symbols, SNa-rH1; open symbols, ventricular myocytes.

voltages from −42 mV to −2 mV from selected pairs of SNa-rH1 cells and ventricular myocytes which had similar voltage dependence of activation. Over this voltage range, the kinetics of Na^+ currents were nearly identical in SNa-rH1 cells and in rat ventricular myocytes (Fig. 1*A*). Peak Na^+ currents were recorded near −20 mV, and the Na^+ currents reversed in direction near +70 mV in these cells (Fig. 1*B*).

For comparison of the average voltage-dependent properties of Na^+ channels in several cells, conductance–voltage relationships were determined from the current–voltage relationships and averaged for multiple cells (Fig. 1*C*). In the whole-cell configuration, the voltage for half-maximal steady-state activation, $V_{1/2}$, was −32.4 ± 3.7 mV (n = 4) in SNa-rH1 cells and −36.0 ± 2.6 mV (n = 5) in ventricular myocytes. For steady-state inactivation, $V_{1/2}$ was −61.9 ± 3.3 mV in SNa-rH1 cells (n = 4), compared with $V_{1/2}$ of −60.5 ± 6.2 mV in ventricular myocytes (n = 6) (Fig. 1*C*). The slopes of the activation and inactivation curves for the two cell types were also similar (see k values in the legend of Fig. 1*C*). The voltage-dependent properties of the Na^+ currents in

these two cell types were also compared in the cell-attached configuration, because the results from the whole-cell configuration might be influenced by the dialysis of the intracellular compartment of the cell or by imperfect voltage clamp of the large, rapid Na^+ currents in ventricular myocytes and SNa-rH1 cells. As in the whole-cell configuration, the voltage dependence of activation and inactivation and the reversal potentials were the same within the error of the measurements (Fig. 1*D*; see Fig. 3 *C* and *D* for original traces).

The nearly identical properties of the expressed and native Na^+ currents recorded in the whole-cell and cell-attached configurations indicate that they are due to the same channel type and are consistent with other reports of rat cardiac Na^+ channel properties (1, 2, 18–20). Evidently, the α subunit of the rH1 Na^+ channel is sufficient to specify its major functional properties when stably expressed in mammalian cells as here or when transiently expressed (21), as previously shown for brain and skeletal muscle Na^+ channels (16, 22).

Modulation of Na^+ Currents of SNa-rH1 Cells and Ventricular Myocytes by Activation of PKC. Regulation of cardiac Na^+ channels by PKC was studied in the cell-attached configuration of the patch clamp technique to preserve the integrity of the intracellular milieu. Addition of the PKC activator OAG (1-oleoyl-2-acetyl-*sn*-glycerol) to the bath solution produced a dose-dependent reduction of peak Na^+ current in both SNa-rH1 cells and primary cultured rat cardiac myocytes (Fig. 2). At a holding potential of −114 mV, the average reduction in SNa-rH1 cells was 33.2 ± 21.0% ($n = 9$, $P < 0.05$) at 10 μM OAG and 66.0 ± 18.0% ($n = 3$, $P < 0.05$) at 100 μM OAG (Fig. 2*A*). No changes in Na^+ current kinetics were observed (see scaled traces in Fig. 2*B*), in contrast to the slowed inactivation observed after OAG treatment of rat brain and skeletal muscle Na^+ currents (9, 10).

The high-Ca^{2+}, high-Cl^- solutions used in the experiments of Fig. 2 *A* and *B* were chosen because they are the same as those used previously to study brain and skeletal muscle Na^+ channels. However, cardiac myocytes beat spontaneously in this solution, making recordings difficult. When extracellular Ca^{2+} was lowered to 1 μM (1 mM Ca^{2+} and 1.15 mM EGTA) or under nominally Ca-free conditions (10 μM Ca^{2+} and 1.15 mM EGTA), 10 μM OAG produced an initial slowing of Na^+ current inactivation and a subsequent reduction of peak amplitude in the cardiac myocytes, as we had previously observed in brain and skeletal muscle cells (Fig. 2*D*). In some myocytes (4 out of 13 cells), this slowing persisted even after peak current was reduced, while in others (9 out of 13) it was transient. In contrast to the results in myocytes, when SNa-rH1 cells were studied in low-Ca^{2+} solutions, 10 μM OAG decreased the peak amplitude of cardiac Na^+ current without altering inactivation kinetics (Fig. 2*C*). Thus, the low-Ca^{2+}, low-Cl^- solutions revealed an OAG-induced slowing of Na^+ current inactivation in cardiac myocytes but not in SNa-rH1 cells. These solutions were used for the remainder of the experiments reported here.

Altered Voltage Dependence of Steady-State Inactivation After Activation of PKC by OAG. OAG effects on voltage-dependent properties were similar in the two cardiac preparations (Fig. 3 *A* and *B*). The voltage dependence of steady-state activation was not altered by OAG (Fig. 3 *A* and *B*). However, the voltage dependence of steady-state inactivation determined with 98-ms prepulses was shifted significantly in the hyperpolarized direction by 10 μM OAG [≈14 mV in SNa-rH1 cells (Fig. 3*A*) and ≈8 mV in ventricular myocytes (Fig. 3*B*)]. Since the voltage dependence of inactivation overlaps the normal range of diastolic potentials in

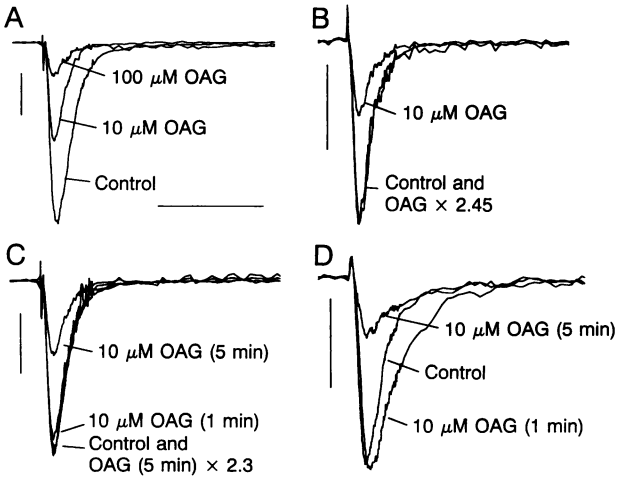

FIG. 2. Modulation of cardiac Na^+ channels by OAG. (*A*) Na^+ currents in a cell-attached patch on a SNa-rH1 cell in response to depolarizations to −16 mV from a holding potential of −116 mV before and after 5-min exposure to the indicated OAG concentrations in the high-Ca^{2+}, high-Cl^- solutions. (*B*) A similar experiment with a ventricular myocyte. (*C*) Na^+ current in a SNa-rH1 cell in response to depolarizations to −14 mV from a holding potential of −114 mV before and after exposure to the indicated concentrations of OAG in the low-Ca^{2+}, low-Cl^- solution with 1.0 μM free Ca^{2+}. (*D*) A similar experiment with a ventricular myocyte. Calibration: 4 ms, 10 pA.

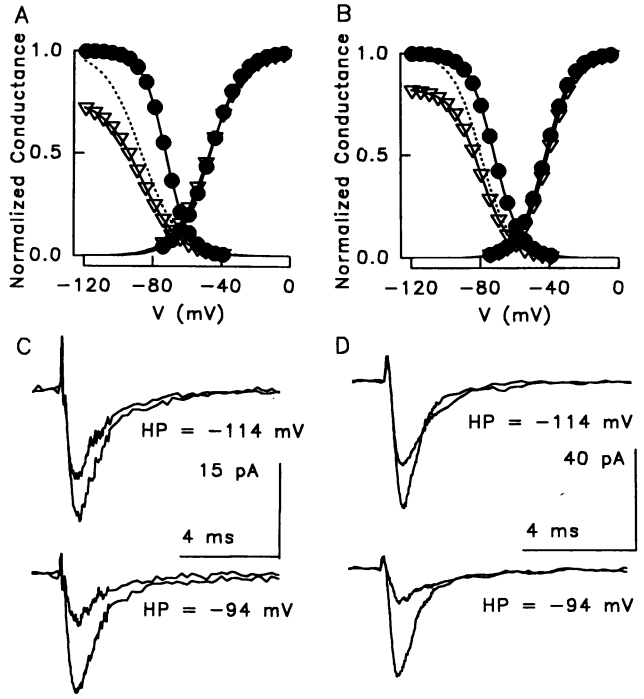

FIG. 3. Shift of the voltage dependence of steady-state inactivation and reduction of maximum Na^+ current by treatment with OAG. (*A*) Average steady-state Na^+ current solution and inactivation curves from SNa-rH1 cells in control solution (filled symbols) and after 10 min in the presence of 10 μM OAG (open symbols). Average curves were constructed as described for Fig. 1*C*. The dotted lines are the scaled versions of inactivation curves in the presence of OAG. The parameters for the Boltzmann relationships in control are the same as in Fig. 1*D*, and in 10 μM OAG are the following for SNa-rH1 cells: $V_{1/2}$ for activation is −47.2 ± 7.9 mV with $k = -10.0$ ± 2.3 mV ($n = 8$); and $V_{1/2}$ for inactivation is −86.8 ± 12.9 mV with $k = 10.9$ ± 2.2 mV ($n = 8$). (*B*) A similar series of experiments in cardiac myocytes: $V_{1/2}$ for activation is −40.6 ± 5.1 mV with $k = -7.8$ ± 0.8 mV ($n = 7$); and $V_{1/2}$ for inactivation is −79.2 ± 2.4 mV with $k = 8.3$ ± 0.3 mV ($n = 5$). (*C*) Effects of holding potential on OAG action. Na^+ currents elicited in a SNa-rH1 cell by depolarizations to −14 mV from the indicated holding potentials (HP) before (larger current in each pair) and during (smaller current) exposure to 10 μM OAG. (*D*) A similar experiment in a ventricular myocyte.

cardiac myocytes, this effect of OAG on the voltage dependence of inactivation would be expected to produce a significant reduction in Na^+ current at normal diastolic potentials. To examine this point, we measured the voltage dependence of Na^+ current reduction by 10 μM OAG after changes in holding potential (>1 min). In SNa-rH1 cells (Fig. 3*C*), the 33% reduction in Na^+ current observed in test pulses from a holding potential of −114 mV was increased to 56 ± 27% at a holding potential of −94 mV ($n = 9$, $P < 0.05$). In primary cultured cardiac myocytes (Fig. 3*D*), the reduction was 35 ± 22% at −114 mV ($n = 6$) and 49 ± 24% at −94 mV ($n = 6$, $P < 0.05$). The reduction in Na^+ current test pulses from a holding potential of −134 mV was similar to −114 mV in SNa-rH1 cells (36 ± 20%, $n = 4$, data not shown), indicating that maximal Na^+ current was observed at a holding potential of −114 mV. Thus, 10 μM OAG reduced Na^+ current in cardiac cells by ≈33% at a holding potential of −114 mV and by considerably greater amounts at normal diastolic potentials.

Inhibition of the Effects of OAG by a Peptide Inhibitor of PKC. To test whether the effect of OAG on the cardiac Na^+ channel was due to activation of PKC, SNa-rH1 cells were microinjected with an inhibitory peptide corresponding to the pseudosubstrate site of PKC (PKCI). After injection with a 500 μM solution of this peptide, exposure to 10 μM OAG for 10 min had no significant effects on Na^+ current (Fig. 4*A*; mean Na^+ current reduction was 3.4 ± 4.1% at holding potential of −114 mV, $n = 4$). In contrast, application of 10 μM OAG to cells that had been microinjected at least 10 min earlier with a peptide inhibitor of cAMP-dependent protein kinase (PKI) gave the normal reduction in sodium current (Fig. 4*B*; 34 ± 7% at −114 mV, $n = 4$). This indicates that, at the concentrations used in this study, OAG effects on cardiac Na^+ channels can be attributed solely to the activation of PKC and that cAMP-dependent protein kinase was not involved.

Single-Channel Recordings from SNa-rH1 Cells. Single Na^+ channels recorded from cell-attached patches on SNa-rH1 cells at voltages from −70 to −20 mV had a conductance of 11 pS. Channels opened early during step depolarizations and then inactivated (Fig. 5*A*). After exposure to 10 μM OAG (Fig. 5*B*), the single channel conductance was identical and the channel opening pattern was little changed. As expected from our whole-cell recordings, opening frequency was reduced, resulting in a decrease in the ensemble averaged current without affecting current time course (Fig. 5 *C* and *D*). In brain and skeletal muscle Na^+ channels, the reduction of Na^+ current in OAG was associated with failure of inactivation, resulting in prolonged bursts of openings during long depolarizations in a substantial fraction of depolarizations (9, 10). To detect such Na^+ channel behavior in SNa-rH1 cells, we counted sweeps containing channel openings after 5 and 10 ms of depolarization. In 560 sweeps, such late openings were seen after 5 ms in 44.6% of traces and after 10 ms in 20.0% of traces in control. In comparison, late openings were observed after 5 ms in 34.3% and after 10 ms in 17.1% of 560 traces in OAG. Therefore, OAG does not increase the number of late channel openings for rH1 Na^+ channels. Its effects on peak Na^+ currents in SNa-rH1 cells can be attributed solely to decreased probability of opening in response to depolarization.

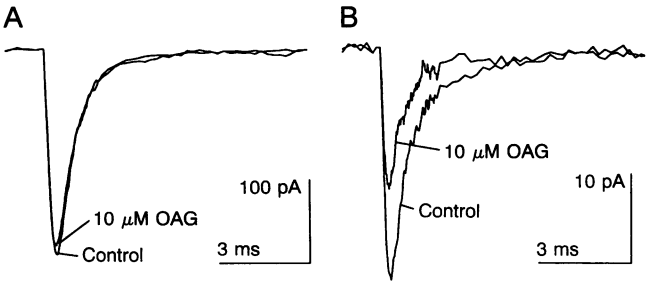

FIG. 4. Effect of OAG in SNa-rH1 cells requires PKC activation. (*A*) Effect of 10 μM OAG on Na^+ current in a SNa-rH1 cell that had been microinjected with PKCI more than 10 min earlier. (*B*) Effect of 10 μM OAG on Na^+ current in a cell that had been microinjected with PKI more than 10 min earlier. Currents were elicited by depolarizations to −14 mV from a holding potential of −114 mV.

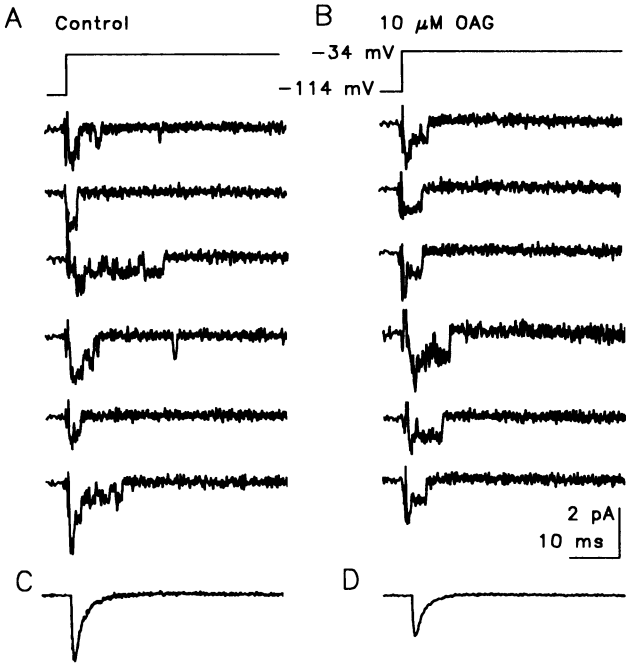

FIG. 5. Effects of OAG on activity of single Na^+ channels in SNa-rH1 cells. (*A*) Recordings from a cell-attached patch containing 4 active channels during pulses to −34 mV from a holding potential of −114 mV before exposure to 10 μM OAG. (*B*) Recordings from the same cell after treatment with 10 μM OAG. (*C*) Ensemble average of 28 traces before exposure to OAG. (*D*) Ensemble average of 28 traces after exposure to OAG. The trace from *D* has been normalized (multiplied by 1.6) and superimposed on the data in *C* to demonstrate the lack of effect of OAG on current time course.

Mechanism of Modulation of Na^+ Channels in Cardiac Muscle Cells by PKC. Activation of PKC reduces cardiac Na^+ current in both cultured ventricular myocytes and SNa-rH1 cells. Reduced activity of single Na^+ channels by OAG at one voltage was observed previously in cultured neonatal cardiac myocytes (23). The decrease in Na^+ current in our experiments was caused by a combination of a hyperpolarizing shift in the voltage dependence of steady-state inactivation and a reduction in peak Na^+ current recorded in test pulses from the most negative holding potentials. This differs from PKC modulation of brain and skeletal muscle Na^+ channels, where the voltage dependence of inactivation is unaffected. The decrease in current observed at holding potentials similar to normal diastolic potentials (e.g., 56% at −94 mV) could dramatically decrease the excitability of cardiac cells.

Our experiments do not indicate which hormones or neurotransmitters can modulate cardiac Na^+ channel function through PKC phosphorylation and thereby reduce myocardial excitability. However, angiotensin II activates PKC in the heart and has multiple modulatory effects on Na^+ currents in cardiac myocytes (23–25). Some of these effects may result from activation of PKC. In addition, our results suggest the presence of additional pathways for modulation of the activity of cardiac sodium channels. We consistently observed that the voltage dependence of activation and especially of steady-state inactivation was more negative in

cell-attached patch experiments than in whole-cell voltage-clamp experiments. This difference may reflect the effects of intracellular regulatory pathways that are disrupted by cellular dialysis in the whole-cell voltage-clamp configuration.

Consistent with previous experiments (23) which did not detect changes in single channel conductance or kinetics with activation of PKC in cardiac myocytes, we observed no slowing of Na^+ channel activation or inactivation kinetics and no delayed openings of single channels in high-Ca^{2+}, high-Cl^- solutions. However, after changing to an extracellular solution containing only 1.0 μM Ca^{2+}, 10 μM OAG caused a transient or maintained slowing of Na^+ current kinetics in addition to the reduction in peak current in cultured cardiac myocytes but not in SNa-rH1 cells. Thus, as for the brain and skeletal muscle Na^+ channels, OAG can slow inactivation of the cardiac Na^+ channel under some conditions.

The molecular mechanism of Na^+ current modulation by PKC in the cardiac Na^+ channel may resemble that for the brain type IIA Na^+ channel. Since similar reduction in peak Na^+ current was observed with native cardiac Na^+ channels in ventricular myocytes and with only the α subunit expressed in SNa-rH1 cells, the α subunit alone is sufficient for this aspect of modulation by PKC. In the rat brain type IIA Na^+ channel α subunit, mutation of serine-1506 in a consensus sequence for PKC phosphorylation prevents both the slowing of inactivation and the reduction of peak Na^+ current associated with PKC phosphorylation (14). This site is in a short, highly conserved intracellular loop between homologous domains III and IV that serves as the inactivation gate. Mutation of another serine residue in the intracellular loop between homologous domains I and II in the rIIA α subunit blocks OAG-induced reduction of peak Na^+ current, but inactivation of Na^+ current is still slowed (26). These results with the rIIA Na^+ channel indicate that serine-1506 is responsible for slowing of inactivation and that phosphorylation at serine-1506 is also necessary for reduction of Na^+ current by phosphorylation at a second site in the intracellular loop between homologous domains I and II. The consensus sequence surrounding serine-1506 (Ser-1505 in the rH1 channel; ref. 3) is unaltered in the rH1 Na^+ channel. Presumably this site is also involved in PKC modulation of the cardiac Na^+ channel. However, the structure of the intracellular loop between domains I and II differs substantially between the rIIA and rH1 α subunits. Studies of site-directed mutants of phosphorylation sites in the rH1 Na^+ channel will provide further insights into the molecular basis for the modulatory effects of PKC on this channel.

We thank Dr. Martha Bosma for critical comments on the manuscript and Yanling Wang for advice and assistance in establishing the clonal cell line SNa-rH1 and in cell culture. This work was supported by Research Grant P01-HL44948 from the National Institutes of Health to W.A.C. and by a National Research Service Award from Training Grant T32-GM07270 to J.R.

1. Baer, M., Best, P. M. & Reuter, H. (1976) *Nature (London)* **263**, 344–345.
2. Brown, A. M., Lee, K. S. & Powell, T. (1981) *J. Physiol. (London)* **318**, 455–477.
3. Rogart, R. B., Cribbs, L. L., Muglia, L. K., Kephart, D. D. & Kaiser, M. W. (1989) *Proc. Natl. Acad. Sci. USA* **86**, 8170–8174.
4. Kallen, R. G., Sheng, Z.-H., Yang, J., Chen, L., Rogart, R. B. & Barchi, R. L. (1990) *Neuron* **4**, 233–242.
5. Gellens, M. E., George, A. L., Jr., Chen, L. Q., Chahine, M., Horn, R., Barchi, R. L. & Kallen, R. G. (1992) *Proc. Natl. Acad. Sci. USA* **89**, 554–558.
6. Cribbs, L. L., Satin, J. A., Fozzard, H. A. & Rogart, R. B. (1990) *FEBS Lett.* **1**, 195–200.
7. White, M. M., Chen, L., Kleinfeld, R., Kallen, R. G. & Barchi, R. L. (1991) *Mol. Pharmacol.* **39**, 604–608.
8. Linden, D. J. & Routtenberg, A. (1989) *J. Physiol. (London)* **419**, 95–119.
9. Numann, R., Catterall, W. A. & Scheuer, T. (1991) *Science* **254**, 115–118.
10. Numann, R. E., Hauschka, S. D., Scheuer, T. & Catterall, W. A. (1992) *Biophys. J.* **61**, 112 (abstr.).
11. Sigel, E. & Baur, R. (1988) *Proc. Natl. Acad. Sci. USA* **85**, 6192–6196.
12. Dascal, N. & Lotan, I. (1991) *Neuron* **6**, 165–175.
13. Schreibmayer, W., Dascal, N., Lotan, I., Wallner, M. & Weigl, L. (1991) *FEBS Lett.* **291**, 341–344.
14. West, J. W., Numann, R., Murphy, B. J., Scheuer, T. & Catterall, W. A. (1991) *Science* **254**, 866–868.
15. Drugge, E. D., Rosen, M. R. & Robinson, R. B. (1985) *Circ. Res.* **57**, 415–423.
16. West, J. W., Scheuer, T., Maechler, L. & Catterall, W. A. (1992) *Neuron* **8**, 59–70.
17. Hamill, O. P., Marty, A., Neher, E., Sakmann, B. & Sigworth, F. J. (1981) *Pflügers Arch.* **391**, 85–100.
18. Kunze, D. L., Lacerda, A. E., Wilson, D. L. & Brown, A. M. (1985) *J. Gen. Physiol.* **86**, 691–719.
19. Ono, K., Fozzard, H. A. & Hanck, D. A. (1993) *Circ. Res.* **72**, 807–815.
20. Zhang, J.-F., Robinson, R. B. & Siegelbaum, S. A. (1993) *Neuron* **9**, 97–103.
21. O'Leary, M. E., Chahine, M., Chen, L. Q., Kallen, R. G. & Horn, R. (1993) *Biophys. J.* **64**, 91 (abstr.).
22. Ukomadu, C., Zhou, J., Sigworth, F. J. & Agnew, W. S. (1992) *Neuron* **8**, 663–676.
23. Benz, I., Herzig, J. W. & Kohlhardt, M. (1992) *J. Membr. Biol.* **130**, 183–190.
24. Nilius, B., Tytgat, J. & Albitz, R. (1989) *Biochim. Biophys. Acta* **1014**, 259–262.
25. Moorman, J. R., Kirsch, G. E., Lacerda, A. & Brown, A. M. (1989) *Circ. Res.* **65**, 1804–1809.
26. Numann, R., West, J. W., Li, M., Smith, R. D., Goldin, A. L. & Catterall, W. A. (1992) *Soc. Neurosci. Abstr.* **18**, 1133.